Liquid Crystals
Publication details, including instructions for authors and subscription information:
http://www.informaworld.com/smpp/title~content=t713926090

The relationship between formation kinetics and microdroplet size of epoxy-based polymer-dispersed liquid crystals

George W. Smith[a]; Nuno A. Vaz[a]
[a] Physics Department, General Motors Research Laboratories, Warren, Michigan, U.S.A.

To cite this Article Smith, George W. and Vaz, Nuno A.(1988) 'The relationship between formation kinetics and microdroplet size of epoxy-based polymer-dispersed liquid crystals', Liquid Crystals, 3: 5, 543 — 571
To link to this Article: DOI: 10.1080/02678298808086401
URL: http://dx.doi.org/10.1080/02678298808086401

LIQUID CRYSTALS, 1988, VOL. 3, NO. 5, 543–571

The relationship between formation kinetics and microdroplet size of epoxy-based polymer-dispersed liquid crystals

by GEORGE W. SMITH and NUNO A. VAZ
Physics Department, General Motors Research Laboratories Warren, Michigan 48090-9055, U.S.A.

(*Received 2 October 1987; accepted 24 December 1987*)

Polymer films containing dispersions of liquid crystal microdroplets have considerable potential for use in displays and other light control devices. These polymer-dispersed liquid crystal (PDLC) films operate by electric field control of light scattering, rather than by polarization control as in the case of twisted nematic systems. The scattering characteristics of the PDLC films are determined by the refractive indices of the polymer and liquid crystal and by the size of the microdroplets. We have found that it is possible to regulate the microdroplet size by controlling the droplet formation rate (i.e. the cure kinetics of the film). Using calorimetry and scanning electron microscopy, we determined the influence of cure kinetics on microdroplet size for epoxy-based PDLCs. We found that droplet size increased with increasing cure time constant. However, the relationship changed as cure temperature was varied, perhaps as a result of competing cure processes. We also determined the phase behaviour of the epoxy-based PDLCs. The liquid crystal acted as a plasticizer, depressing the glass transition temperature of the PDLC samples slightly below that of the pure epoxy. The temperature and enthalpy of the nematic to isotropic transition of the liquid crystal material in the microdroplets were both functions of cure temperature. From the transition enthalpy it was possible to estimate α, the fraction of liquid crystal contained in the droplets; we found that α decreased with increasing cure temperature, presumably as a result of greater liquid crystal solubility in the epoxy matrix at higher temperatures.

1. Introduction

Polymer-dispersed liquid crystal (PDLC) film, consisting of micron-sized liquid crystalline droplets dispersed in a polymer matrix, show considerable promise for flat panel displays, and other light control applications [1–5]. These films can be rapidly (~ 10 ms) switched from a light-scattering state to a transparent one by electric fields on the order of 10^4 V/cm (~ 30 volts across a 20 μm film). The mechanism for formation of the microdroplets will be discussed below.

The operation of PDLC films has been described elsewhere [1–3], but it is worthwhile to summarize the basic principles at this time. The polymer matrix is optically isotropic with refractive index, n_p; the liquid crystal in the microdroplets is optically uniaxial with ordinary and extraordinary indices, n_o and n_e. In the off-state (no applied field), the polymer-liquid crystal interaction at each microdroplet interface determines the configuration of the liquid crystal director within the droplet. In general, this configuration is not uniform within each droplet or from droplet to droplet [1]. As a result, incident light rays probe a range of refractive index values between n_o and n_e. Since $n_o \neq n_e$, these indices cannot all be equal to the polymer index n_p, and incoming light is multiply scattered by the microdroplets. Upon application of an electric field

strong enough to overcome the interactions at the droplet boundaries, the liquid crystal directors reorient along the field direction (usually normal to the film). In this case light incident normal to the film probes essentially the ordinary refractive index of the liquid crystal in the droplets. We choose the liquid crystal and polymer so that n_o matches n_p fairly well. As a result, incident light will detect no optical change at the liquid crystal/droplet boundary, and no scattering will occur; the film will be transparent.

It is clear from this discussion that PDLC films have several potential advantages when compared to twisted nematic cells. Since the basis of operation is light scattering rather than polarization control, no polarizers are required. Furthermore, since the active medium is a solid polymer rather than a liquid, it is easier to fabricate films on polymer substrates coated with transparent conductors. Thus large, flexible light control films are possible.

The electro-optic properties of PDLC films obviously depend on liquid crystal microdroplet size since the scattering is most efficient when the droplet size matches the wavelength of incident light. Furthermore, control of the indices is optimized and efficient use of the liquid crystal material is maximized if all the liquid crystal is confined to the droplets, and none is dissolved in the polymer matrix. Therefore, in order to control both of these factors, it is important to understand the process whereby the liquid crystal microdroplets are formed.

A qualitative model we have developed suggests that film formation kinetics and liquid-crystal/polymer mutual solubilities play an important role in determining microdroplet size, and hence electro-optic properties. A faster formation rate would be expected to yield smaller microdroplets. The mechanism of droplet formation is complex. However, there is considerable evidence that a phase separation process is involved. Initially a liquid polymer precursor and the liquid crystal are stirred together to produce a homogeneous mixture. Subsequently the polymer matrix is hardened†. During the hardening the solubility of the liquid crystal in the matrix decreases so that tiny droplets of liquid crystal separate from the polymer‡. Evidence for a similar process has been put forth for epoxy-elastomer systems [6]. There is some evidence that spinodal decomposition may be the phase separation mechanism in polymer–polymer systems [7].

In order to understand the formation processes of PDLC films, it is important to determine the relationship between formation time and droplet size. We have undertaken a study to determine this relationship using calorimetric methods and electron microscopy. We investigated a thermoset system in which the matrix was an epoxy and the liquid crystal a biphenyl mixture. For a thermoset the droplet formation would be governed by the time required for cure. In other words, the formation time constant would essentially equal that for the cure process. However, only one time constant is directly measurable—that for cure.

2. Experimental aspects

2.1. *Materials*

The epoxy matrix used in the present study was a three-component mixture of Devcon 5A resin, Epon 812 resin, and Capcure 3-800 hardener in 1 : 1 : 2 volumetric

† Hardening may take place either by curing (for thermosets) or by cooling from the melt or solvent evaporation (for thermoplastics).

‡ Some droplet coalescence may also be involved in the early stages of formation (before gelation).

proportions. We used two resins in equal proportions in order to achieve close index matching to the liquid crystal†. In some cases a very small concentration (< 1 per cent) of an accelerator‡ (Capcure EH-30) was added to the Capcure 3-800 to increase the rate of cure (see § 3.1*c* below). This small amount of accelerator (< 0·5 per cent of the total epoxy composition; < 0·33 per cent of the total PDLC film composition) produced a negligible change in the refractive index. Properties of the epoxy components are given in table 1.

Table 1. Sample components.

Component name	Concentration range	Density g/cm^3	Refractive index†
Devcon 5A Resin	1 part	1·156	1·5723
Epon 812 Resin	1 part	1·228	1·4832
Capcure 3-800 Hardener	2 parts	1·122	1·5015
Capcure EH-30 Accelerator	0, 0·25, 0·5, 1·0 Vol. Pct. in 3-800‡	0·9653	1·5148
E7 Liquid crystal	0 or 2 parts	1·0095	1·5258 (n_o) 1·7399 (n_e)

† Refractive index values determined at 25°C.

‡ These values correspond to 0, 0·125, 0·25, and 0·5 volume per cent accelerator in epoxy samples or 0, 0·083, 0·167, and 0·333 volume per cent accelerator in epoxy liquid-crystal samples.

Note: n_o = ordinary index; n_e = extraordinary index.

The liquid crystal chosen for this work was E7, a four-component mixture of substituted biphenyls and a terphenyl [8]. Properties of E7 are also listed in table 1. The mixture is in its nematic liquid crystalline phase at temperatures up to 333·4 K. In the present study, for reasons of time and simplicity, only one liquid crystal concentration was used: 33·3 volume per cent.

2.2. *Experimental methods*

(1) *Calorimetry*. Calorimetric techniques proved extremely valuable in determining two types of experimental information: kinetics and energetics of the cure process, and phase behaviour of both the cured polymer matrix and the cured PDLC. The

† The refractive indices of Devcon A, Epon 812, and Capcure 3-800 are, respectively, 1·5723, 1·4832, and 1·5046. Thus an uncured 1 : 1 : 2 mixture of the three has an index of 1·5146. Since some residual liquid crystal remains in the matrix after polymerization, the refractive index of the cured mixture is found to match very well the ordinary refractive index (1·5258) of the biphenyl liquid crystal (E7 from BDH Chemicals, a subsidiary of E. Merck).

‡ The relationship between x, the volume per cent of accelerator in the Capcure 3-800 hardener, and A, the volume per cent hardener in the total sample volume (either epoxy or epoxy/liquid-crystal) is given by $A = x/(2 + L/H + 0{\cdot}01x)$, where L/H is the ratio of liquid crystal volume to that of the hardener in the sample. Thus, for a given value of x, the values of A for samples with and without liquid crystal are unequal.

experimental procedures for measuring isothermal cure kinetics have been briefly discussed elsewhere [9], and phase behaviour determination methods have also been previously described [2, 3]. However, it will be useful to review both techniques in greater detail at this time.

(*a*) *Sample preparation.* Samples for calorimetric studies were prepared by mixing appropriate amounts of epoxy resin plus hardener (which may or may not contain accelerator) and, if desired, liquid crystal. To achieve suitable mixing it was necessary to stir the various components together for at least 30 seconds. The epoxy precursors chosen cured very slowly at room temperature; therefore, the time required for mixing had little effect on the subsequent cure kinetics measurement. Some air bubbles were introduced into the samples during the mixing process, but their presence was felt to be relatively unimportant to the cure process.

The amount of each component required to prepare a mixture was typically on the order of 20 to 25 μl, as measured using precision disposable micropipettes. Thus the total volume of mixtures was on the order of 100 μl. Of this, only about 10 μl ($\sim$ 10 to 12 mg), again measured by a micropipette, was required for a calorimetric run. Samples were pipetted into an aluminium sample pan which was hermetically sealed, weighed to a precision of 0·01 mg (for a total sample weight on the order of 10 mg), and transferred to a Perkin–Elmer DSC-2 Differential Scanning Calorimeter for the kinetics measurement. The temperature and atmosphere in the calorimeter were precisely controlled: temperatures were regulated to better than 0·1 K; the ambient atmosphere was nitrogen, flowing into the calorimeter dry box at about 5 ml/s.

(*b*) *Measurement of isothermal cure kinetics and energetics.* Our calorimetric determination of cure kinetics involved the measurement of the rate of heat evolved (exothermic power) during isothermal cure. If the cure proceeded exponentially, the rate constant (or time constant) could be determined either by a semi-logarithmic plot or by using the Mangelsdorf method of analysis [9]. As we shall see (§ 3.1) the cure of epoxy-based systems generally departed appreciably from exponential behaviour.

A sealed sample of uncured epoxy (or epoxy plus liquid crystal) was placed in the calorimeter sample holder at room temperature (300 K), and the temperature programmed rapidly (320 K/min) to the desired cure temperature. The time dependence of the exothermic power, dQ/dt, was then recorded using the calorimeter computer's isothermal software (DSCI). The heat release was followed until the cure process was essentially complete. The total heat release could be calculated by an integration of the heat release curve, using the DSCI software (this same software could also be used to determine a partial heat release during any part of the cure process).

We measured the heat release for four types of epoxy-based systems: epoxy resin plus hardener, resin plus hardener with accelerator, resin plus hardener plus liquid crystal, and resin plus hardener/accelerator plus liquid crystal. Cure kinetics were followed at temperatures ranging from 325 K to 425 K.

(*c*) *Measurement of phase behaviour.* The calorimeter also enabled us to determine the phase behaviour of the cured samples. For these measurements the D.S.C. was operated in its temperature scanning mode, in which the sample temperature was programmed linearly over a range of interest while changes in the sample's heat absorption rate were monitored. In the case of a cured epoxy film with no liquid crystal, the glass transition temperature and its associated heat capacity change were measured. For an epoxy-plus-liquid-crystal sample (i.e. a PDLC sample) the

nematic–isotropic transition temperature and enthalpy could also be determined (in addition to the glass transition parameters).

Figure 1 (*a*) compares the D.S.C. thermal spectra for an epoxy and an epoxy-based PDLC†. The epoxy sample exhibits a single transition—a change in the D.S.C. baseline level over a 10 to 15 degree temperature range. This baseline level change is due to a change in sample heat capacity (ΔC_p) associated with the epoxy's glass transition, at which the polymer sample changes from a brittle low temperature state to a more flexible high temperature one.

Although the transition occurs over a range of temperature, it is convenient to define a single temperature—the glass transition temperature, T_g—at which the change is said to occur. A reasonable estimate of T_g is taken to be the temperature at which the D.S.C. curve is half-way between extrapolated tangents to the baselines above and below the transition region.

The D.S.C. curve for the PDLC sample is a bit more complex. In addition to a glass transition, two small endothermic peaks are observed (first order phase transformations). The one at lower temperature is apparently a residual peak due to liquid crystal melting; the higher temperature one corresponds to the clearing point (nematic to isotropic transition) of liquid crystal in the PDLC microdroplets. A comparison of the PDLC D.S.C. curve to that for the pure liquid crystal (figure 1 (*b*)) shows that the melting peak is appreciably shifted to lower temperature and reduced in area. On the other hand, the peak due to the clearing point, while broadened, is only slightly shifted and reduced. This difference in behaviour is, of course, ascribable to the fact that impurities depress the melting temperature according to rules governing eutectic-forming systems, whereas the nematic–isotropic transition temperature obeys different laws—those of liquid–liquid transformations. This purity effect is discussed more fully in § 4.3.

The epoxy-based systems investigated herein do not exhibit residual melting peaks since the E7 liquid crystal mixture generally forms a glass rather than a crystalline solid at low temperatures. Thus it was not possible to extract values of melting temperatures or enthalpies for these materials. However, from the area and temperature (at maximum deflection) of the clearing point peak we determined the enthalpy (ΔH_{NI}) and temperature (T_{NI}) of the nematic–isotropic transition (see § 3.2 (2)).

For some samples phase behaviour scans were repeated after the passage of some time to determine whether aging produced measureable effects. In addition, phase behaviour studies were also repeated after post-cure heat treatments to discover their effect.

(2) *Scanning electron microscopy (SEM) studies.* In order to determine the size of the liquid crystal microdroplets (expected to lie in the 0·1 to 10 μm range) we recorded scanning electron micrographs of a number of PDLC samples cured in the calorimeter‡.

† The D.S.C. scans in figure 1 are for illustrative purposes only. The epoxy and liquid crystal materials used to obtain them are different from the systems investigated in this paper. In fact, the liquid crystal of figure 1 is single component system, whereas E7 is a mixture (see above). Single component liquid crystals generally exhibit melting peaks in their D.S.C. spectra while multi-component mixtures often form glasses and thus do not yield melting peaks.

‡ Thus, the cure temperature and formation kinetics of these samples were well controlled and much better known than for any PDLC samples previously studied by SEM.

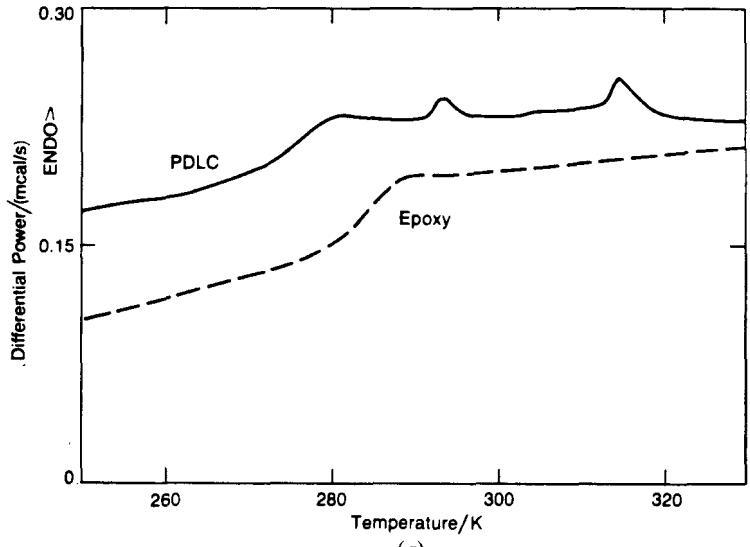

(*a*)

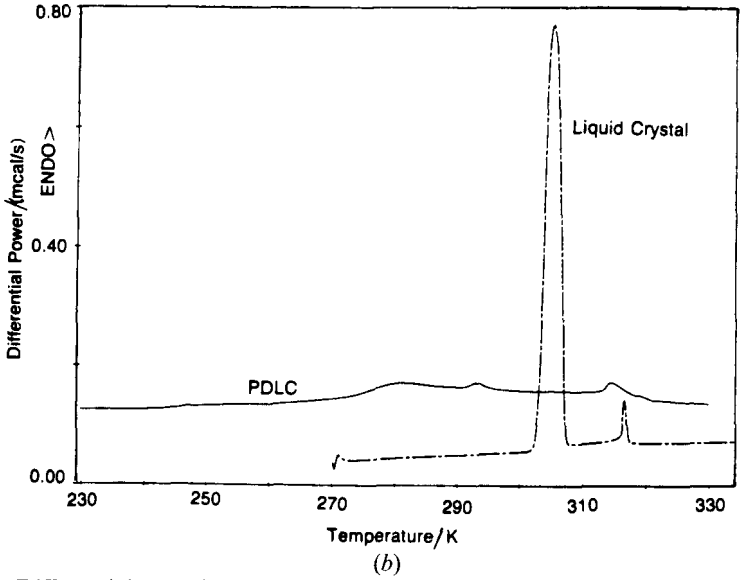

(*b*)

Figure 1. Differential scanning calorimetry thermal spectra of epoxy, epoxy/liquid-crystal (PDLC), and liquid crystal samples: (*a*) Comparison of epoxy and PDLC samples. The pure epoxy exhibits only a glass transition—a heat capacity change at temperature T_g. The PDLC sample glass transition is shifted to lower temperature by the plasticizing action of the liquid crystal remaining in the epoxy matrix; the two peaks are associated with the liquid crystal. (*b*) Comparison of PDLC and pure liquid crystal samples. The two small PDLC peaks are due to the melting and clearing point transitions and are shifted with respect to those of the pure, single component liquid crystal (in this example *p-n*-heptyl-cyanobiphenyl).

The procedure for obtaining the SEM images involved the following steps: (1) the hermetic seal of the aluminum sample pan was removed and the pan sides folded down for access to the specimen; (2) the cured sample was removed from the D.S.C. pan and glued to an aluminium SEM stud; (3) a section of the sample was removed from the sample top using a razor blade in order to achieve a flat surface for

examination; (4) the stud was placed in a sputtering unit which was evacuated to approximately 20 mtorr of Hg for at least one hour (this process removed essentially all of the liquid crystal from the microdroplets exposed by the cutting step); (5) the sample was coated with a thin Au–Pd coating to provide the conductive surface required for the SEM; (6) the sample mounted on the stud was then placed in the SEM and examined at magnifications up to 8000×, using an acceleration potential of 15 kV.

3. Results

3.1. *Cure kinetics studies*

(1) *Effect of temperature on cure process.* As mentioned above (§ 2.2 (1 *b*)) isothermal cure behaviour was studied for epoxy-based systems at temperatures from 325 K to 425 K. Over that range the cure process changed considerably. In the next two sections we shall examine the behaviour of epoxy cure in samples with and without the addition of liquid crystal (and without accelerator). We shall then describe the effect of accelerator on the cure behaviour.

(*a*) *Epoxy samples—no liquid crystal, no accelerator.* Temperature has a significant effect on the character of the epoxy cure process. This is readily apparent from an examination of the heat release curves of figure 2. In the figure the exothermic power† is plotted vs. time elapsed after the cure temperature was reached (following the rapid scan from 300 K)‡. Results for four different temperatures are shown, and two major temperature-dependent aspects are clear: (1) The overall time required for completion of cure is dramatically reduced as the temperature increases from 325 K to 400 K. (2) The shape of the heat release curves changes drastically from 'non-ideal' behaviour at 325 K to almost exponential time dependence at 400 K§. It should be added that a further increase in cure temperature to 425 K does not appreciably change the cure behaviour from that observed at 400 K.

It is not the purpose of the present work to examine in detail the reasons for this temperature-related change in behaviour. However, two competing reactions are apparently involved [10, 11]. At lower temperatures the two processes occur at different rates, leading to the complex heat release curve shapes. At high temperatures, both processes are rapid, resulting in a more nearly exponential behaviour. One of the reactions undoubtedly involves active hydrogen from the thiol components of the curing agent; the other may be homopolymerization. A significant aspect of the cure curves is the fact that the most noticeable change in cure character seems to occur between 325 K and 350 K. This point will be relevant to our discussion of the influence of cure kinetics on microdroplet size (see § 4.1 (1)).

Since the cure curves are complex, it is not possible to derive meaningful kinetics parameters using the Mangelsdorf method. A useful cure kinetics parameter can, however, be assigned for each curve by defining the cure time constant, τ_{max}, to be the

† By convention exothermic curves are plotted as downward-going.

‡ We re-emphasize the fact that the time to reach the cure temperature was negligible compared to the overall cure time.

§ An ideal exponential heat release curve (see [21]) would exhibit an instantaneous onset of the exotherm, followed by an exponential return to the zero-release baseline. In practice, of course, the initial rise is more gradual, due to instrumental factors and sample-related considerations. Thus in figure 2 the curve for 400 K exhibits a fast, but not instantaneous onset, followed by a more-or-less exponential decay.

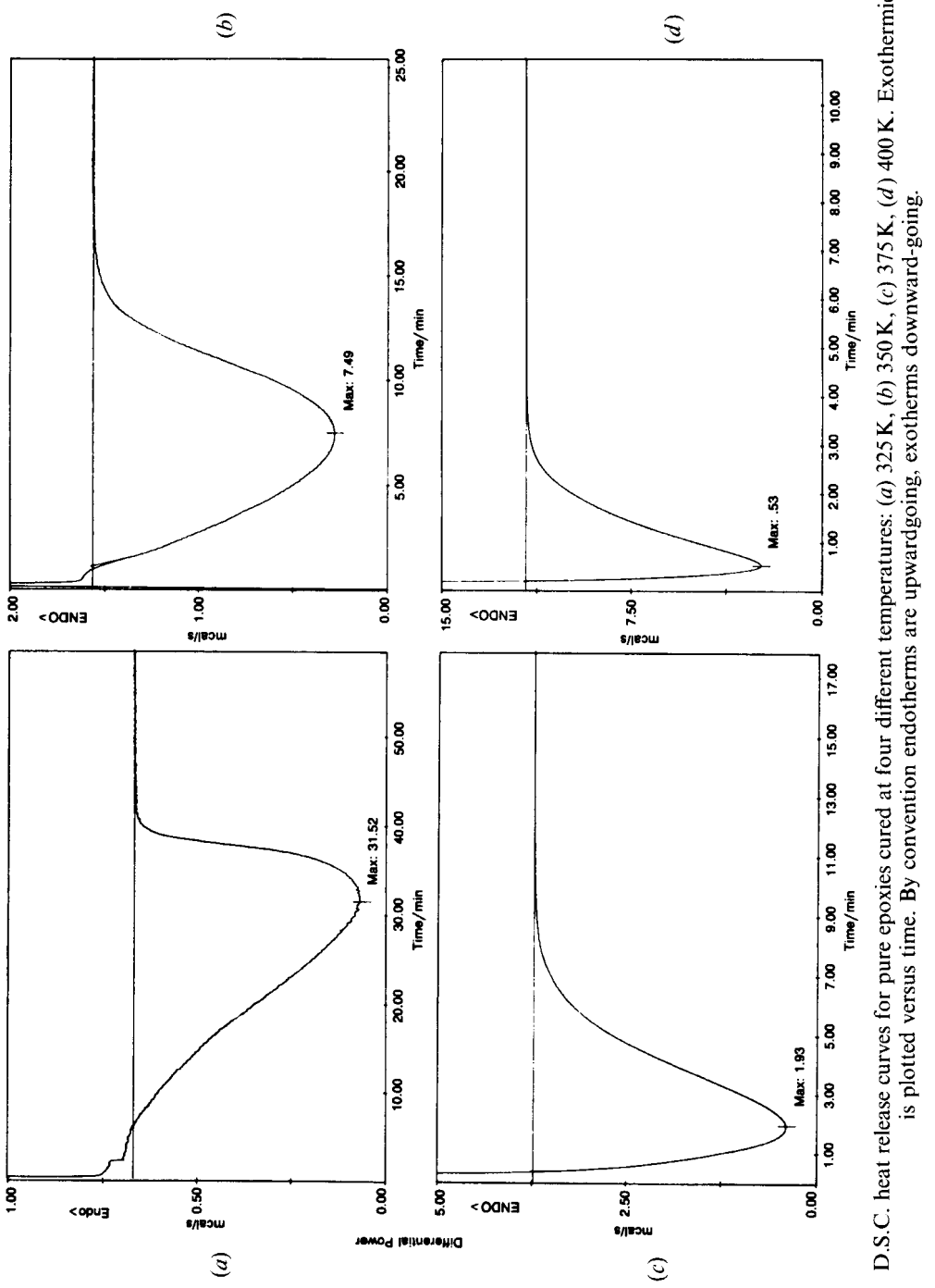

Figure 2. D.S.C. heat release curves for pure epoxies cured at four different temperatures: (*a*) 325 K, (*b*) 350 K, (*c*) 375 K, (*d*) 400 K. Exothermic power is plotted versus time. By convention endotherms are upwardgoing, exotherms downward-going.

time for maximum rate of heat release for that curve. The reasonableness of this procedure will be seen below when Arrhenius plots of τ_{max} are examined: values of τ_{max} and total heat release will be tabulated (§ 3.1(1 *d*)).

(*b*) *Epoxy plus liquid crystal—no accelerator.* The addition of liquid crystal to the epoxy precursor material leads to somewhat slower cure rates, as expected for a diluent. However, the temperature-dependent change in the character of the heat release curves shows a behaviour similar to that for the pure epoxy samples. This is apparent from an examination of cure curves for some epoxy/liquid-crystal samples (figure 3). As in the case for the undiluted epoxy, the cure curves show the largest change in character between 325 K and 350 K.

As above we defined τ_{max} to be the time for maximum of heat release for each curve. Derived kinetics parameters will be tabulated below.

(*c*) *Effect of accelerator on cure behaviour.* We studied the effect of accelerator concentration on cure behaviour at various temperatures between 325 K and 425 K for epoxy samples both with and without liquid crystal. Although addition of accelerator did increase cure rate, the shape of the cure curves for both types of sample did not change very much with increasing accelerator concentration for each temperature within the entire range. This fact is illustrated in figure 4 for epoxy cure curves and in figure 5 for epoxy/liquid-crystal cures. This apparent insensitivity of cure character to accelerator concentration (A) provided us with a reliable way to control cure kinetics for our study of the influence of microdroplet formation rate on droplet size. If we held temperature constant and varied A, neither the cure character nor the mutual solubilities of the components varied from one experiment to another—both of which would change if we varied temperature in order to control kinetics.

(*d*) *Summary of cure data.* The results of the cure experiments are summarized in table 2 which is divided into two parts. The first part lists cure kinetics parameters for epoxy precursors with varying accelerator concentrations and no liquid crystal; the second part gives results for the same epoxy samples plus 33·3 volume per cent liquid crystal. Due to dilution the volume per cent of accelerator is, of course, lower for samples containing liquid crystal. The nature of the cure curve shape is given in the table by an appropriate figure number (e.g. 4(*a*) indicates that the heat release curve is similar to that in figure 4(*a*); 3(*b*)/(*c*) suggests that the shape is intermediate to that in figures 3(*b*) and 3(*c*)). Values of ΔQ_{tot}, the total heat release during cure; τ_{max}, the effective cure time as determined from the time for maximum heat release; and τ_{end}, the time by which cure is completed, are listed. It should be emphasized that the value of τ_{end} is approximate since it is difficult to precisely determined from the heat release curves the time by which cure is complete (see figures 2–5). It should be noted that for lower cure temperatures the value of τ_{max} becomes close to that for τ_{end}, indicating a rather anomalous cure behaviour (see, for example, figure 3(*a*)).

The effects of accelerator, temperature, and liquid crystal on the cure time constant, τ_{max}, are more readily seen by plotting τ_{max} as a function of x, the volume per cent accelerator added to the Capcure 3-800.† Such a plot is given in figure 6. It is clear from the figure that increases in either temperature or accelerator content tend to

† It should be re-emphasized that x is not equal to A, the volume percent accelerator in the total sample. As discussed in § 2.1 above, for a given x-value, the corresponding A-values for samples with and without liquid crystal differ from each other (see, for example, table 2.)

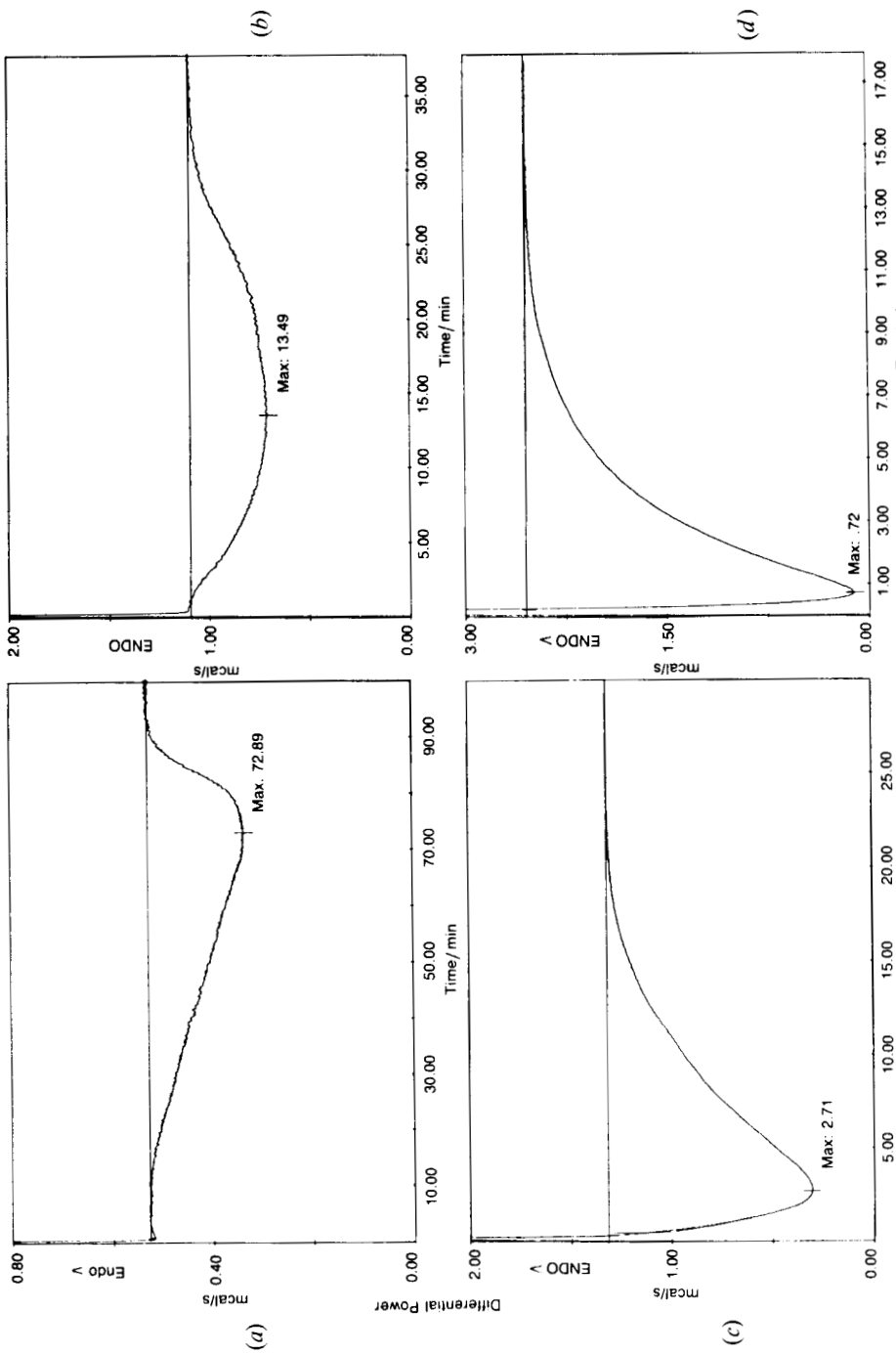

Figure 3. D.S.C. heat release curves for epoxy/liquid-crystal samples cured at four different temperatures: (*a*) 325 K, (*b*) 350 K, (*c*) 375 K, (*d*) 400 K.

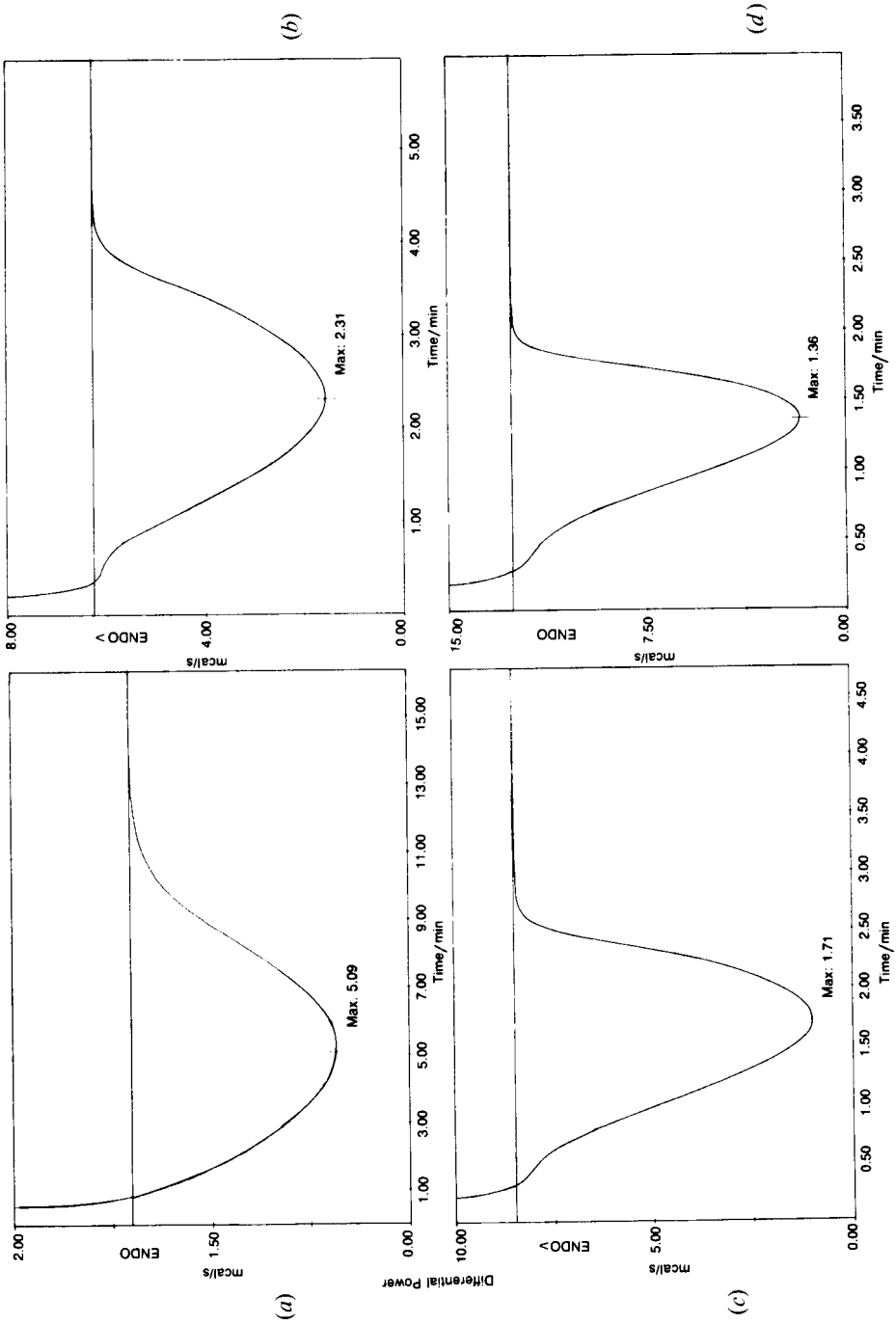

Figure 4. Heat release curves for 362·5 K cure of epoxy samples with various accelerator concentrations, A (volume per cent): (*a*) 0, (*b*) 0·125, (*c*) 0·25, (*d*) 0·5.

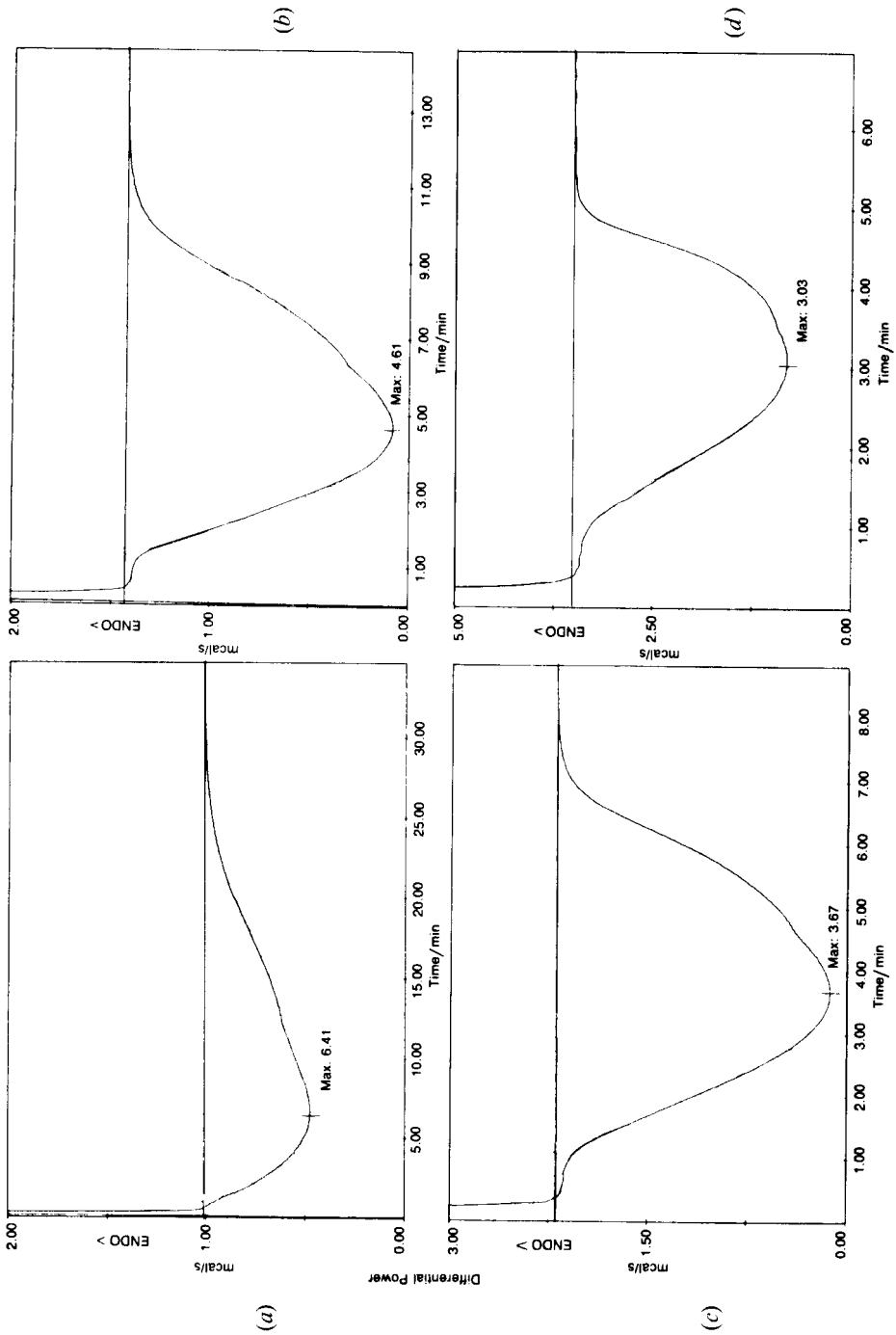

Figure 5. Heat release curves for 362·5 K cure of epoxy/liquid-crystal samples with various accelerator concentrations, A (volume per cent) (*a*) 0, (*b*) 0·083, (*c*) 0·167, (*d*) 0·333.

Table 2. Cure kinetics parameters for epoxy-based samples.

A, Accel. conc. (Vol. Pct.)†	Cure temp. K	Curve type‡	ΔQ_{tot}/cal/g	τ_{max}/s	τ_{end}/s
No liquid crystal					
0	325·0	2(*a*)	59·24	1890	2500
0	350·0	2(*b*)	57·11	450	1020
0	362·5	4(*a*)	54·86	305	780
0	375·0	2(*c*)	61·04	116	690
0	400·0	2(*d*)	56·36	32	240
0	425·0	2(*d*)	52·20	16	140
0·125	325·0	2(*a*)	51·37	829	1140
0·125	350·0	2(*b*)	56·59	217	390
0·125	362·5	4(*b*)	55·71	139	270
0·125	375·0	2(*c*)	58·29	70	210
0·25	325·0	2(*a*)	43·85	471	690
0·25	350·0	2(*b*)	49·35	145	240
0·25	362·5	4(*c*)	53·64	103	180
0·25	375·0	2(*b*)/(*c*)	56·81	56	138
0·5	325·0	3(*a*)	54·40	457	660
0·5	350·0	3(*a*)	53·67	135	200
0·5	362·5	4(*d*)	52·21	82	130
0·5	375·0	3(*b*)/(*c*)	51·34	41	90
With 33·3 vol. pct. liquid crystal					
0	325·0	3(*a*)	41·47	4370	5600
0	350·0	3(*b*)	42·12	810	2100
0	362·5	5(*a*)	38·95	385	1800
0	375·0	3(*c*)	42·58	163	1350
0	387·5	3(*c*)/(*d*)	41·42	71	900
0	400·0	3(*d*)	41·88	43	900
0	412·5	3(*d*)	39·29	22	480
0	425·0	3(*d*)	37·96	19	480
0·083	325·0	3(*a*)	41·62	2030	2580
0·083	350·0	3(*b*)	40·67	466	1020
0·083	350·0	3(*b*)	39·09	570	1140
0·083	350·0	3(*b*)	41·11	570	1200
0·083	362·5	5(*b*)	38·32	277	750
0·083	375·0	3(*c*)	41·65	142	600
0·083	400·0	3(*d*)	41·28	43	300
0·167	325·0	3(*a*)	38·93	1370	1740
0·167	350·0	3(*b*)	40·32	393	720
0·167	362·5	3(*c*)	39·69	220	480
0·167	375·0	3(*c*)	41·19	121	390
0·167	400·0	3(*c*)/(*d*)	39·38	40	230
0·333	325·0	3(*a*)	41·63	1260	1560
0·333	350·0	3(*a*)/(*b*)	39·41	366	530
0·333	362·5	5(*d*)	38·18	182	330
0·333	375·0	3(*b*)/(*c*)	37·30	84	250
0·333	400·0	3(*c*)/(*d*)	39·68	37	160

† *A* = volume per cent accelerator in total sample volume.

‡ Curve type refers to the heat release curve in the indicated figure number. Thus, 3(*a*) indicates that the heat release curve for the sample is similar to that in figure 3(*a*); 3(*a*)/(*b*) indicates that the heat release curve is intermediate to that of figures 3(*a*) and 3(*b*).

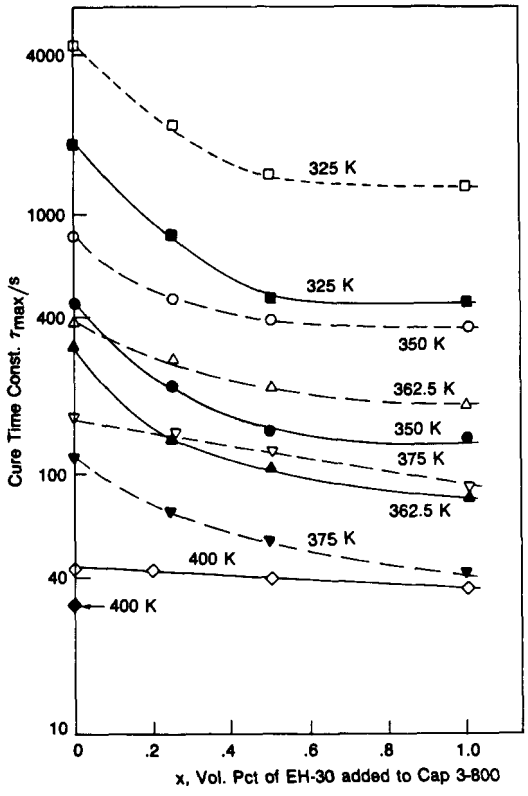

Figure 6. Effect of cure temperature, accelerator concentration, and liquid crystal content on cure time constant τ_{max}, as determined from the time for maximum heat release rate. Solid curves are for pure epoxy samples, dashed curves for epoxy/liquid-crystal samples. Cure temperatures are indicated for each curve.

reduce the cure time constant, whereas addition of liquid crystal increases the time constant. However, the effect of accelerator saturates at very low values of x.

In order to test whether τ_{max} is a reasonable approximation to the cure time constant, we constructed Arrhenius plots of τ_{max} versus reciprocal temperature for each sample series with a constant accelerator concentration (both with and without liquid crystal). The results for $x = 0$ ($A = 0$) are shown in figure 7. The linear behaviour for both curves suggests that the time for maximum heat release is, indeed, a suitable parameter with which to estimate cure kinetics. The greater slope (larger activation energy) for the epoxy/liquid-crystal combination shows that dilution inhibits the cure process. Arrhenius plots for the samples with other accelerator concentrations also show good linearity. Activation energies derived from cure time constants for the four series of samples (i.e. four different accelerator concentrations) are given in table 3.

It is apparent from table 2 that measured values of ΔQ_{tot} vary to some extent (from 43·85 to 61·04 for pure epoxies, from 37·3 to 42·58 for epoxy/liquid-crystal samples). Such variations may be due, in part, to sample-to-sample variations (perhaps as a result of incomplete mixing of the components). However, other contributing factors may include incomplete cure or (for fast cure times) partial cure during the rapid warmup to the cure temperature. Any heat-release during the warmup would not be

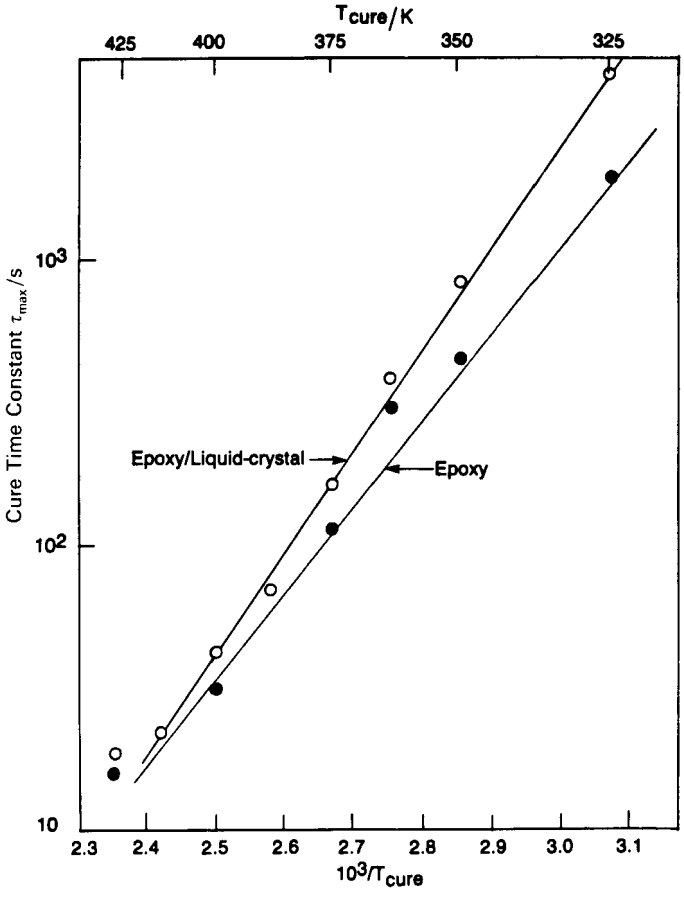

Figure 7. Arrhenius plot of τ_{max} for epoxy samples with and without liquid crystal and no accelerator. Activation energies for the two curves are 14·0 kcal/mole (epoxy) and 16·2 kcal/mole (epoxy/liquid-crystal).

Table 3. Activation energies from Arrhenius plots of τ_{max}.

x, Accel. conc.† (Vol. Pct.)	*A*, Accel. conc.‡ (Vol. Pct.)	Activation energy (kcal/mole)
No liquid crystal		
0	0	14·0
0·25	0·125	12·0
0·5	0·25	10·3
1·0	0·5	11·7
With 33·3 vol. pct. liquid crystal		
0	0	16·2
0·25	0·083	13·2
0·5	0·167	12·2
1·0	0·333	12·5

† x = volume per cent accelerator in Capcure 3-800 hardener.
‡ A = volume per cent accelerator in total sample volume.

included in the computed heat of cure; this would be a negligible consideration for slow cure kinetics. In spite of the variations, meaningful average values of ΔQ_{tot} were obtained: 54·3 ± 4·0 cal/g for the epoxies, 40·2 ± 1·5 cal/g for epoxy/liquid-crystal samples. The fact that the value of ΔQ_{tot} for the PDLC samples is a larger fraction of the epoxy value than expected from dilution considerations (0·74 rather 0·67) suggests that the epoxy value of ΔQ_{tot} may be a bit low; a magnitude of about 60 cal/g (roughly the maximum observed epoxy value) would be consistent with the measured value of 40·2 cal/g for the PDLC samples. However, reduction of ΔQ_{tot} by dilution may not be a linear function of diluent. Published cure heats for epoxies range from 27 to 91 cal/g [12].

3.2. *Phase behaviour*

As we have seen in the illustrative example of figure 1, the phase behaviour of a cured epoxy sample is quite simple: a glass transition identified by a change in heat capacity (i.e. a change in D.S.C. baseline). A cured epoxy/liquid-crystal sample, on the other hand, exhibits a nematic–isotropic transition peak, as well as a glass transition somewhat depressed below the epoxy T_g (due to plasticizing action of the liquid crystal).

(1) *Glass transition.* Our studies indicate that the glass transition parameters of the pure epoxy samples are relatively insensitive to both accelerator concentration, A, and cure temperature, T_{cure}; therefore, it is sufficient to show a single D.S.C. scan for a typical epoxy sample (figure 8). The first part of table 4 lists the glass transition temperatures and associated heat capacity changes ($\Delta C_p/m$) for epoxies cured with four different accelerator concentrations at various cure temperatures. The values of heat capacity change are normalized by divison by the sample mass.

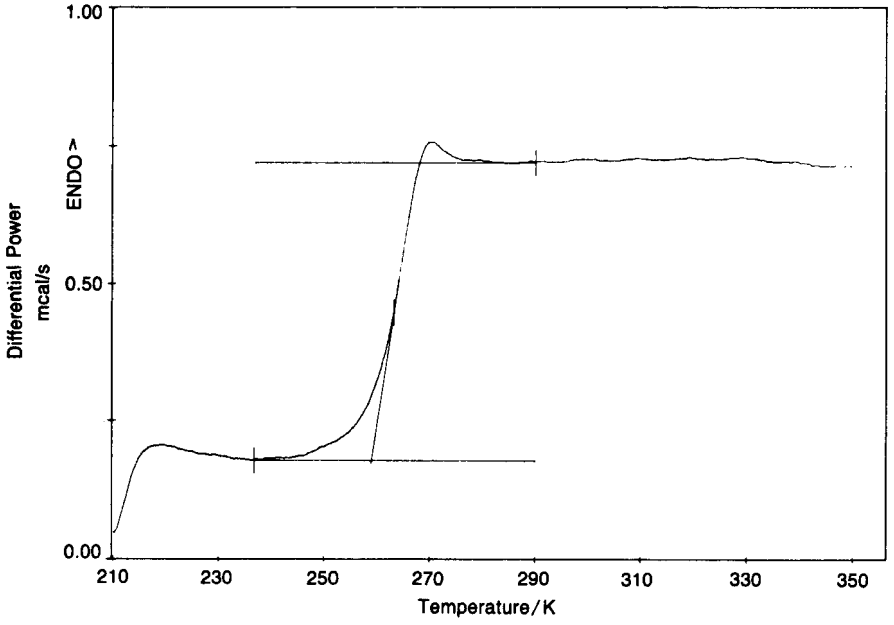

Figure 8. D.S.C. thermal scan for epoxy sample cured at 362·5 K. Differential power is plotted versus temperature. The shift in baseline is due to a heat capacity change associated with the glass transition at 263 K.

Table 4. Phase behaviour parameters for epoxy-based samples.

A (Vol. Pct.)	T_{cure} (K)	T_g (K)	$\Delta C_p/m$ (cal/g-deg)	T_{NI} (K)	ΔH_{NI} (cal/g)
No liquid crystal					
0	325·0	262·9	0·1444	–	–
0	350·0	261·1	0·1518	–	–
0	362·5	266·3	0·1515	–	–
0	375·0	264·5	0·1399	–	–
0	400·0	262·2	0·1330	–	–
0	425·0	263·8	0·1578	–	–
0·125	325·0	261·8	0·1509	–	–
0·125	350·0	262·6	0·1533	–	–
0·125	362·5	262·1	0·1460	–	–
0·125	375·0	263·7	0·1541	–	–
0·25	325·0	261·1	0·1443	–	–
0·25	350·0	261·5	0·1467	–	–
0·25	362·5	263·1	0·1493	–	–
0·25	375·0	264·0	0·1508	–	–
0·5	325·0	264·9	0·1585	–	–
0·5	350·0	263·6	0·1157	–	–
0·5	362·5	263·0	0·1496	–	–
0·5	375·0	263·6	0·1561	–	–
With 33·3 vol. pct. liquid crystal					
0	325·0	260·2	0·1170	319·5	0·305 ± 0·035
0	350·0	259·0	0·1238	319·0	0·26 ± 0·03
0	362·5	260·4	0·1069	321·4	0·21 ± 0·03
0	375·0	260·8	0·1141	325·6	0·165 ± 0·035
0	387·5	259·7	0·1154	325·6	0·165 ± 0·025
0	400·0	261·4	0·0995	327·5	0·10
0	412·5	259·4	0·1067	326·9	0·14 ± 0·03
0	425·0	259·5	0·1000	326·7	0·11
0·083	325·0	259·4	0·1185	317·5	0·275 ± 0·055
0·083	350·0	258·9	0·1173	318·7	0·275 ± 0·035
0·083	350·0	261·1	0·1152	319·8	0·25 ± 0·02
0·083	350·0	260·8	0·1161	319·4	0·27 ± 0·04
0·083	362·5	258·5	0·1110	318·0	0·28 ± 0·06
0·083	375·0	260·7	0·1123	323·0	0·155 ± 0·035
0·083	400·0	260·2	0·1032	324·7	0·11 ± 0·04
0·167	325·0	260·4	0·1183	319·3	0·265 ± 0·035
0·167	350·0	260·1	0·1080	319·5	0·255 ± 0·035
0·167	362·5	259·6	0·1040	319·0	0·25 ± 0·05
0·167	375·0	261·5	0·1013	323·8	0·175 ± 0·025
0·167	400·0	260·3	0·1095	324·9	0·145 ± 0·025
0·333	325·0	261·3	0·1095	319·0	0·285 ± 0·045
0·333	350·0	261·4	0·1087	320·1	0·265 ± 0·045
0·333	362·5	259·4	0·1007	318·6	0·23 ± 0·06
0·333	375·0	260·1	0·1015	321·5	0·20 ± 0·02
0·333	400·0	260·9	0·1125	323·4	0·185 ± 0·025

Note: For pure E7 liquid crystal, T_{NI} = 333·4 K; ΔH_{NI} = 0·91 cal/g.

Values of the glass transition temperature and the associated heat capacity change for epoxy/liquid-crystal samples are given in the second part of table 4. The glass transition temperatures are lower (by a few degrees) than those for the pure epoxy samples. Both T_g and $\Delta C_p/m$ are also fairly insensitive to cure temperature and the

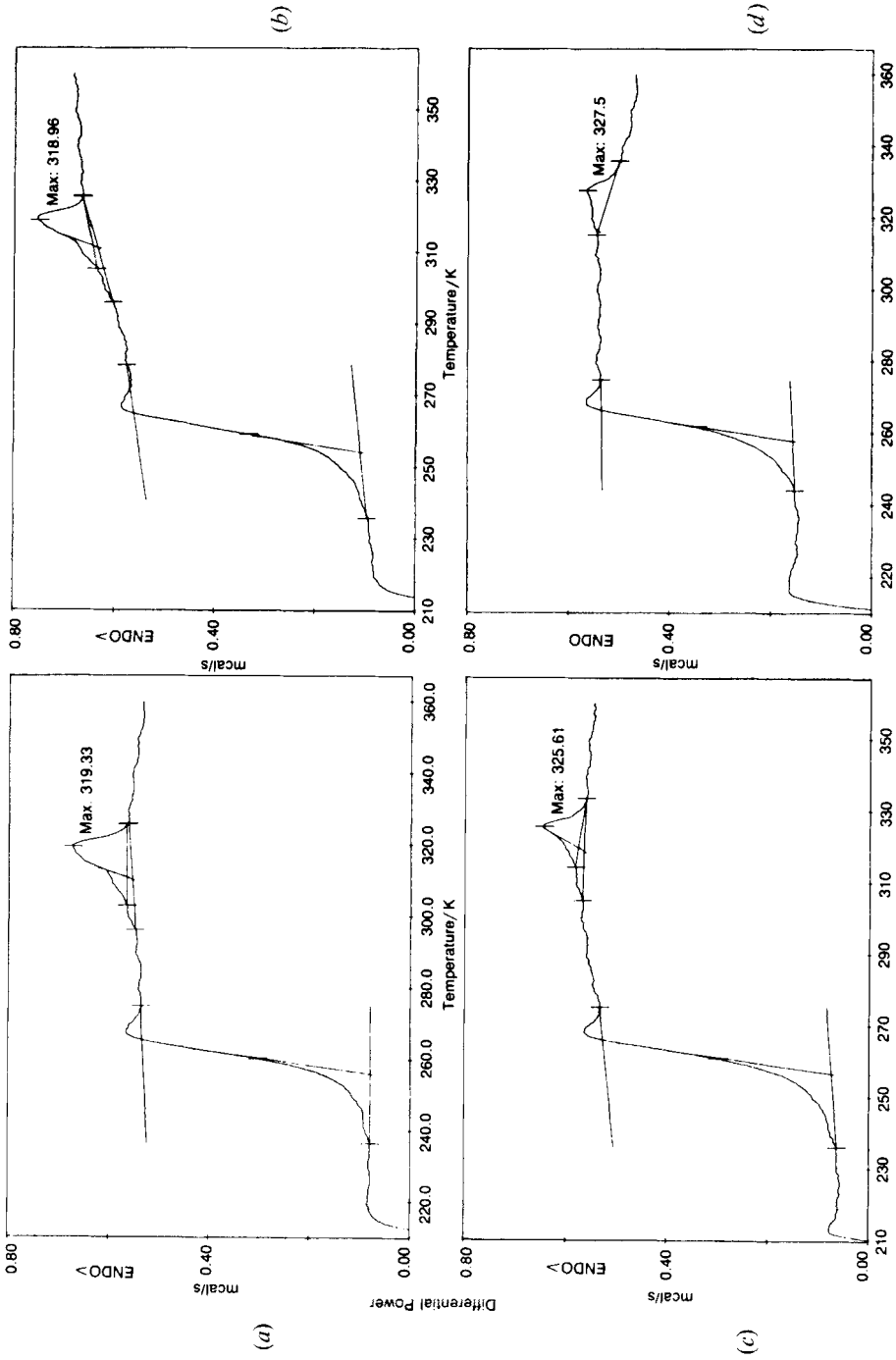

Figure 9. D.S.C. thermal scans for epoxy/liquid-crystal samples cured at various temperatures (no accelerator): (*a*) 325 K, (*b*) 350 K, (*c*) 375 K, (*d*) 400 K. Both the nematic–isotropic temperature and enthalpy are affected by cure temperature: T_{NI} increases, and ΔH_{NI} decreases with increasing T_{cure}. The glass transition temperature is essentially unaffected by cure temperature.

presence of accelerator. Figure 9 shows D.S.C. scans for epoxy/liquid-crystal samples cured at several different temperatures.

(2) *Nematic–isotropic transition.* In contrast to the behaviour of the glass transition, the temperature and enthalpy of the nematic–isotropic transition were found to be affected quite strongly by the cure temperature. This is apparent in figure 9: the peak area decreases and the peak temperature increases as cure temperatures is raised from 325 K to 400 K.

Accelerator concentration has a smaller, but nevertheless noticeable effect on T_{NI} and ΔH_{NI}. Values of the glass transition and nematic–isotropic transition parameters are also given in the second part of table 4.

The influence of accelerator concentration and cure temperature on the transition temperature and enthalpy is made more clear in figures 10 and 11. In figure 10 ΔH_{NI} and T_{NI} are plotted versus A. It can be seen that an appreciable change in behaviour takes place when the cure temperature is increased from 325 K to 400 K. For low cure temperatures the transition temperature and enthalpy values are essentially independent of both accelerator concentration and cure temperature. For cure temperatures above 362·5 K, the transition parameters are somewhat sensitive to T_{cure} and A. The increase in ΔH_{NI} and decrease in T_{NI} with A at the higher cure temperatures is incompletely understood. However, as discussed in § 4.2, the trends seem to suggest

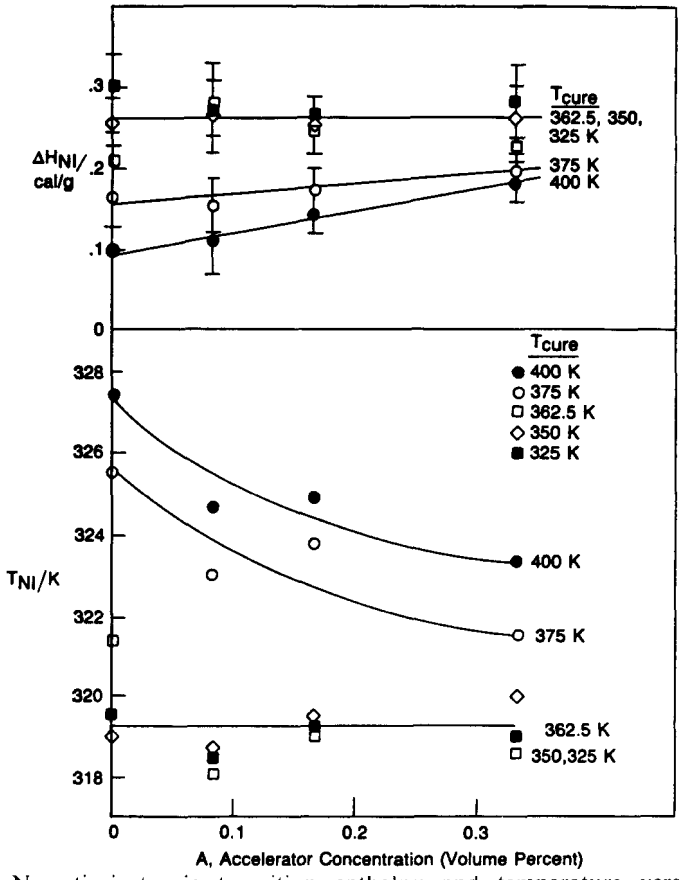

Figure 10. Nematic–isotropic transition enthalpy and temperature versus accelerator concentration for various cure temperatures.

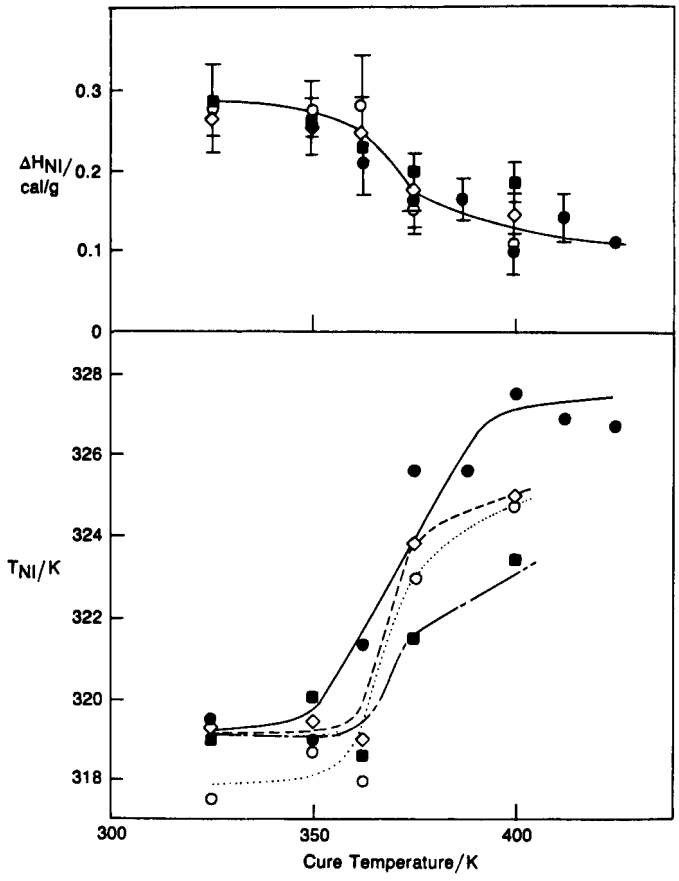

Figure 11. Nematic–isotropic transition enthalpy and temperature versus cure temperature for various values of A, the accelerator concentration (in volume percent): 0 (●), 0·083 (○), 0·167 (◇), and 0·333 (■).

that as A increases, more liquid crystal is trapped in the droplets and that its purity decreases.

The actual dependence on cure temperature is shown in figure 11. The change in behaviour of the nematic–isotropic transition parameters with increasing cure temperature is perhaps not surprising when we recall that the character of the cure process itself shows a dramatic change as cure temperature is increased (see figure 3). The trends of ΔH_{NI} and T_{NI} with increasing cure temperature can be ascribed, we believe, to two effects: the decrease in clearing point enthalpy to a decrease in the amount of liquid crystal contained in microdroplets; the increase in clearing temperature to a higher liquid crystal purity. These points are discussed more fully in § 4.

(3) *Ageing and post-cure effects.* Ageing at room temperature for periods ranging from ten to twenty-seven days shifted the T_g and T_{NI} values of samples both with and without liquid crystal. However, $\Delta C_p/m$ and ΔH_{NI} were unaffected (to within experimental error). For pure epoxy samples ageing shifted T_g to higher temperatures by about 2 K ± 1 K; the shortest ageing period (10 days) produced shifts which averaged a few tenths of a degree smaller. In the case of epoxy/liquid-crystal samples T_g was shifted by 1·4 K ± 0·6 K for all ageing periods.

Ageing also produced positive shifts in the nematic–isotropic transition temperature, but the shift magnitude depended on cure temperature and accelerator concentration. Generally, a low temperature cure led to a larger shift in T_{NI} than that for high temperature cures (see figure 12). This result is reasonable if one supposes that samples cured at low temperatures have a lower degree of cure than those cured at high temperatures; the ageing process would then be expected to produce a greater incremental post cure in the low temperature samples than in the high temperatures ones.

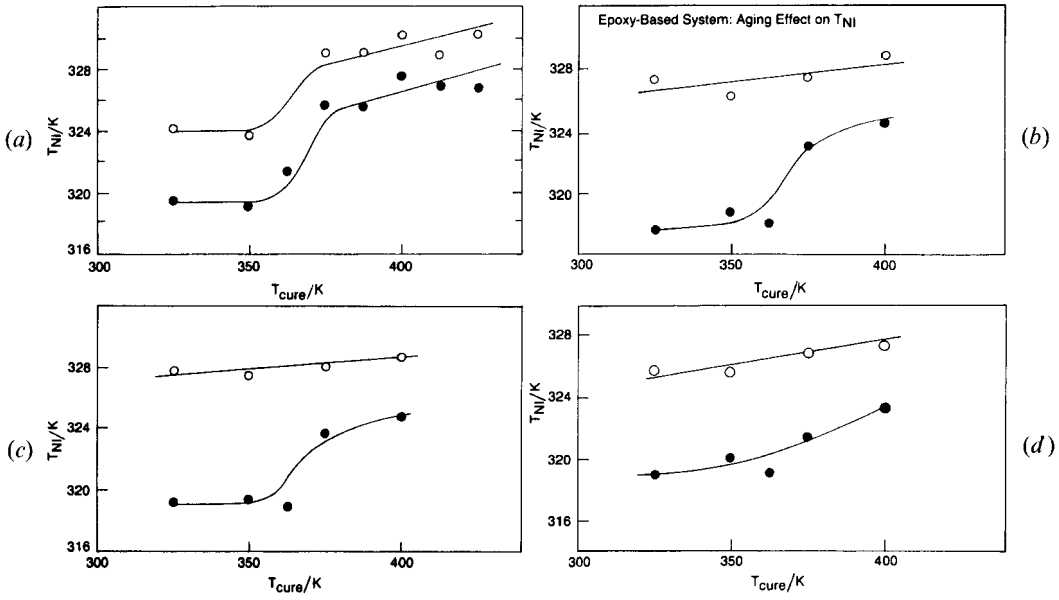

Figure 12. Effect of sample ageing on nematic–isotropic transition temperature; values of A, the accelerator concentration for the four curves are: (*a*) 0, (*b*) 0·083, (*c*) 0·167, and (*d*) 0·333 volume per cent. The filled circles are for samples as initially run, open circles for aged samples.

An accelerated ageing study was carried out by post-curing an epoxy/liquid crystal sample at 400 K for more than 48 hours. The sample (containing 0·083 volume per cent accelerator) was initially cured at 350 K. Immediately following cure, its phase behaviour was determined calorimetrically. The subsequent 400 K post-cure treatment was interrupted periodically for additional D.S.C. scans to be run, yielding values of T_g and T_{NI} as a function of treatment time. The treatment shifted both temperatures to higher values, as expected (see figure 13). T_g increased by about 4 K after almost 50 hours at 400 K; T_{NI} was shifted more than 10 degrees to 332·4 K, a value close to that for E7. On the other hand, $\Delta C_p/m$ and ΔH_{NI} were unaffected by the post treatment.

3.3. *Microdroplet size from scanning electron microscopy*

A typical scanning electron micrograph showing PDLC microdroplets is given in figure 14. It is clear that the droplets are fairly uniform in size and shape, making it relatively easy to estimate droplet diameter. From such micrographs for samples cured at various temperatures and accelerator concentrations, we found that, as predicted, both cure temperature and accelerator concentration produced an appreciable

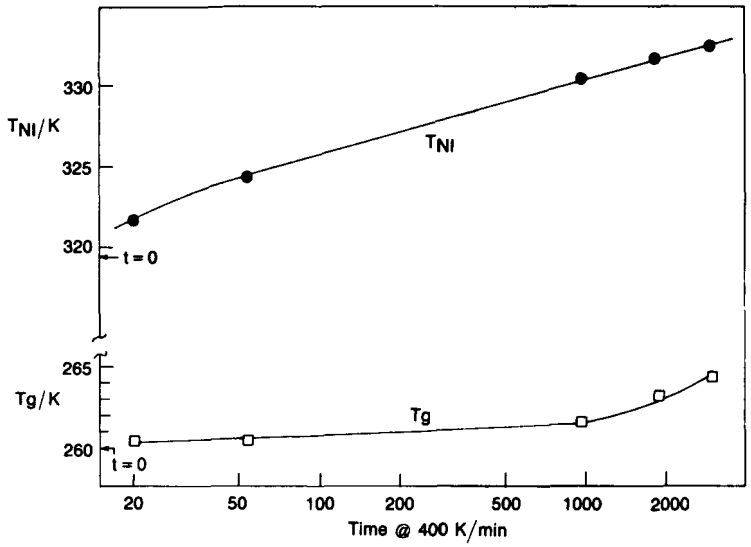

Figure 13. Effect of post-cure treatment at 400 K on nematic–isotropic and glass transition temperatures. T_{NT} and T_g are plotted versus accumulated time at 400 K. T_{NI} for the pure liquid crystal is 333·4 K.

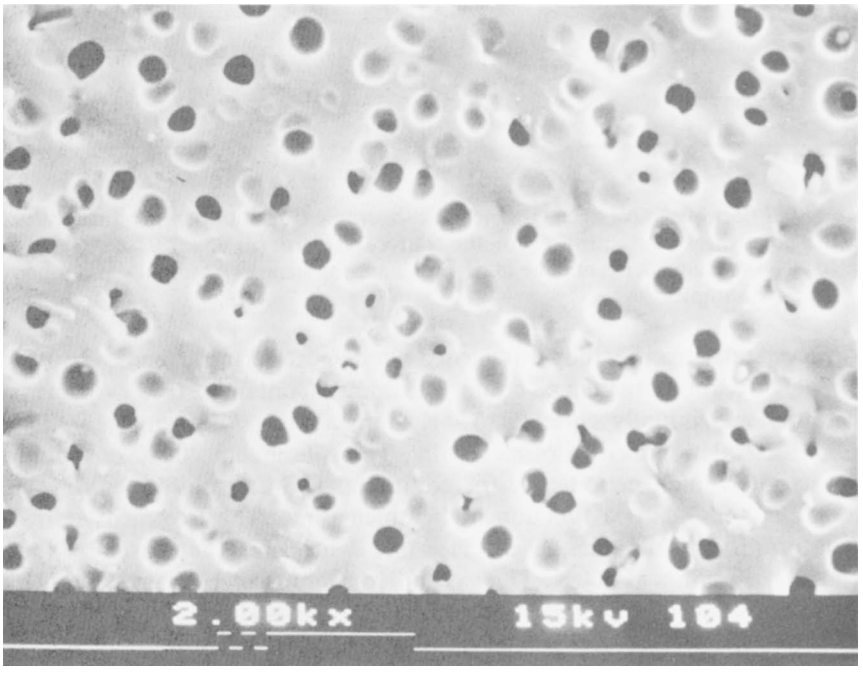

Figure 14. Scanning electron micrograph of PDLC sample cured at 325 K (no accelerator). Typical microdroplets are $\sim 1{\cdot}8\,\mu$m in diameter.

effect on microdroplet size, as seen in figure 15. More meaningful, however, is a plot of droplet diameter as a function of cure time constant, τ_{max} (figure 16). In the figure we see two families of curves, apparently as a result of the change in cure character with increasing cure temperature. We shall discuss this point in §4.1.(1) below.

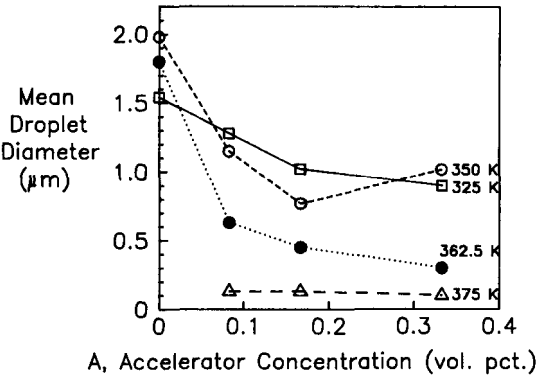

Figure 15. Microdroplet size versus accelerator concentration for various cure temperatures. Cure temperatures for each curve are indicated.

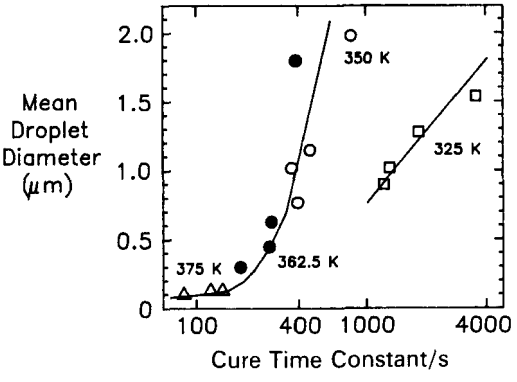

Figure 16. Microdroplet diameter versus cure time constant, τ_{max}. Results are for four different cure temperatures. Cure rate at each temperature was varied by changing the accelerator concentration.

4. Discussion

The primary thrust of this work has been to determine the relationship between cure kinetics (i.e. droplet formation time) and the size of the liquid crystal microdroplets in PDLC films in order to control droplet size and thus optimize electro-optic performance for a given application. We have focused our attention on an epoxy-based system and have succeeded in relating droplet size to kinetic parameters. As expected, the longer the time available for droplets to nucleate and grow during polymerization, the larger the droplet size. However, during this work we also discovered several other factors governing PDLC formation and properties. For instance, from our calorimetric studies we have been able to estimate the fraction of liquid crystal contained within the microdroplets rather than remaining dissolved in the polymer matrix. Let us now summarize our major findings.

4.1. *Effects of cure kinetics and temperature*

As discussed in §3.1(1), the nature of the cure process for both epoxy and epoxy/liquid-crystal samples changed as the cure temperature increased from 325 K

to 400 K due, apparently, to the multiplicity of the chemical reaction mechanisms involved. This change manifested itself in several effects dependent upon cure temperature: (1) a change in the character of the D.S.C. cure heat release curves; (2) a rapid decrease in microdroplet diameter for $T_{cure} > 350$ K; and (3) a shift in T_{NI} and ΔH_{NI}.

Because of the complexities introduced by a cure process which changed markedly with temperature, we had to develop a working definition of cure time constant in order to quantify the cure kinetics of our samples. The most reasonable measure of the time constant seemed to be the time for maximum heat release during cure, τ_{max}. To obtain the widest possible range of cure time constants for a given cure temperature (and also minimize effects due to solubility changes), we added small amounts of accelerator to some samples.

(1) *Microdroplet size.* Our working definition of cure time constant proved adequate to establish a relationship between microdroplet size and cure kinetics, but the resulting plot of droplet diameter versus τ_{max} (figure 16) has two branches: one for $T_{cure} = 325$ K, the other for $T_{cure} \geqslant 350$ K. This duality reflects the change in cure behaviour with increasing cure temperature and the consequent change in the relation of τ_{max} to the true kinetics parameters; for the low temperature branch τ_{max} may be an underestimate of the cure time constant, or for the high temperature branch it may be an overestimate. The fact that the data for 350 K to 375 K fall on a single curve indicates that cure character and solubility effects may not change radically over that temperature range. The increase in droplet diameter with increasing cure time constant is in accordance with our speculation that larger droplets should result when more time is available for 'nucleation' and growth. (Use of the term 'nucleation' does not imply that we rule out the possibility that spinodal decomposition may play a major role in droplet formation.)

The fact that our kinetics studies of epoxy-based systems yielded only a rather arbitrarily defined cure time constant is unsatisfying. To fully understand the droplet formation process we require a simpler polymer system: one for which the cure process follows a simple exponential dependence over a wide range of cure rates with no changes in solubilities. Radiation-cured polymers are excellent candidates to fill these requirements. In particular, ultraviolet-cured systems are most amenable for laboratory study. Using them it is possible to vary cure rate simply by changing the intensity of the U.V. irradiation. This can be done at a constant temperature so that changes in solubility can be avoided. We have begun an investigation of the effect of U.V. cure rate on microdroplet size.

(2) *Clearing point temperature and enthalpy.* As seen in figure 10, both T_{NI} and ΔH_{NI} are affected by cure temperature: the transition temperature is increased and the transition enthalpy decreased for higher values of T_{cure}. The higher value of T_{NI} is presumably due to a more complete cure at high temperature, resulting in less monomer being left to dissolve in the liquid crystalline microdroplets. The presence of monomer as an impurity in the liquid crystal would depress its clearing point. We believe that the decrease in enthalpy indicates that less liquid crystal is present in the form of microdroplets for samples cured at high temperature. This decrease could result from a decrease in the size or number of microdroplets. Faster cure kinetics would certainly reduce droplet size, and greater liquid crystal solubility in the matrix at elevated temperatures could mean that a larger amount of E7 would be retained in the matrix after formation. We can estimate the fraction of liquid crystal in the droplets from calorimetric measurements. The procedure is discussed in the next section.

4.2. *Fraction of liquid crystal in microdroplets*

The fraction, α, of liquid crystal contained in the microdroplets is of interest for several reasons: efficiency of liquid crystal usage during fabrication; influence on optical properties; plasticizer effects; and implications for environmental life. In principle it is possible to estimate α from two calorimetrically determined quantities: the nematic–isotropic transition enthalpy and the glass transition temperature.

(1) *Estimation from* ΔH_{NI}. In order to determine α from ΔH_{NI}, we assume that only the liquid crystal in the microdroplets contributes to the clearing point peak. This is reasonable, since liquid crystal incorporated into the matrix finds itself in an entirely different environment from that of the pure material. In essence, matrix liquid crystal can be regarded as extremely impure; as a result, its clearing peak is so greatly depressed and broadened as to be unobservable. Consequently, the measured value of ΔH_{NI} is reduced below that which would be expected if all the liquid crystal were found in the droplets.

However, two other factors might also help to reduce α: (1) For very small microdroplet size the contribution to the clearing point peak from liquid crystal in the droplets could decrease with increasing surface-to-volume ratio. Depression of T_{NI} and broadening of the associated D.S.C. peak for liquid crystals in submicron pores has been observed by Armitage and Price [13], but they point out that the effect is negligible for pores larger than 1 μm in diameter. Therefore we conclude that droplet size does not appreciably affect α. (2) Monomer retained as an impurity in the liquid crystal would also decrease ΔH_{NI} (and hence α), perhaps by an appreciable amount. We have shown elsewhere [2] that, in the case of a U.V.-cured PDLC system, a few per cent of monomer can reduce the transition enthalpy by as much as 50 per cent. However, in the present case we do not believe impurity to be a major factor since T_{NI} and ΔH_{NI} follow opposite trends with increasing cure temperature (figure 11): as the clearing temperature increases (indicating decreasing impurity content), the enthalpy (and hence the derived value of α) decreases. If purity were the sole consideration, both T_{NI} and ΔH_{NI} would decrease with increasing impurity level.

Under the assumption that only liquid crystal contained in microdroplets contributes to ΔH_{NI}, it is easy to derive the following simple equation for α:

$$\alpha = (1 + F)P, \tag{1}$$

where $F = m_p/m_{lc}$, the ratio of polymer to liquid crystal mass in the sample, and $P = \Delta H_{NI}(\text{obs})/\Delta H_{NI}(\text{lc})$, the ratio of clearing enthalpy measured for the sample to that for the pure liquid crystal. With the volume concentrations and densities given in table 1 and a value of $\Delta H_{NI}(\text{lc}) = 0{\cdot}91 \pm 0{\cdot}06$ [14], equation (1) becomes

$$\alpha = 3{\cdot}573\Delta H_{NI}, \tag{2}$$

Values of α derived from equation (2) are plotted in figure 17 for samples whose thermal spectra were run immediately after curing as well as for aged samples. It is clear that higher cure temperatures markedly reduce α, suggesting that the amount of liquid crystal in the droplets decreases. Figure 17 also shows that ageing does not appreciably change α.

Because of the possibility of an impurity effect, it may be prudent to regard the values of α shown in the figure as a lower limit. However, as discussed above, we feel the impurity effect is small.

(2) *Estimation from* T_g. It is well known among polymer scientists that the addition of small molecules to a polymer can reduce the glass transition temperature; i.e. act

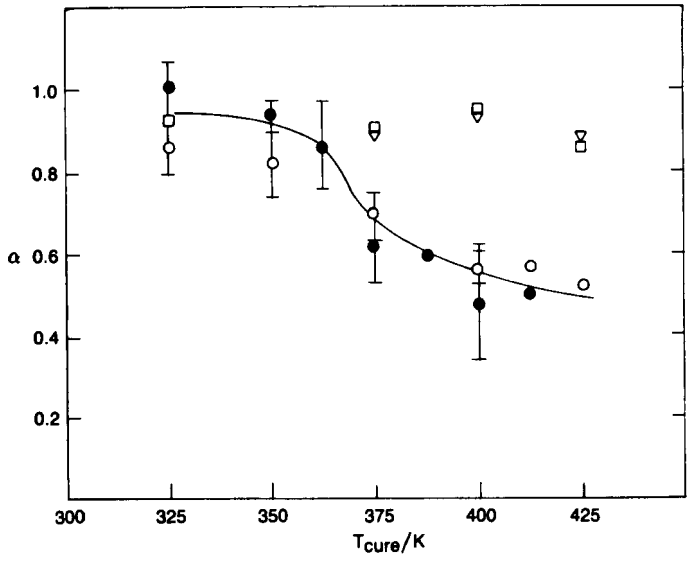

Figure 17. Estimated value of α, the fraction of liquid crystal in the microdroplets, versus cure temperature. Results from transition enthalpy are for samples as initially run (●) and aged samples (○); results from glass transition as initially run (□) and aged samples (▽). As discussed in the text, the enthalpy-derived values are believed to be more reliable.

as a plasticizer. Methods have been proposed to use this effect to determine the amount of low molecular weight component added to the polymer [15, 16]. A simple expression based on the theory of Gordon and Taylor [15] relates the glass temperature, T_g, of a plasticized sample to the weight fractions, W_i, and glass temperatures, T_{gi}, of the pure polymer and pure plasticizer (components 1 and 2 respectively)

$$1/T_g = W_1/T_{g1} + W_2/T_{g2}. \quad (3)$$

Of course, the plasticizer in our case is a liquid crystal. T_g values for certain glass-forming liquid crystal mixtures can be determined calorimetrically [16] and for such low molecular weight systems seem to be on the order of 200 K to 230 K. We ran several D.S.C. scans of E7 which indicated that its T_g lies in the range 204 to 209 K. T_g values for epoxy samples with and without liquid crystal are listed in table 4. Cure temperatures from 325 K to 425 K did not greatly affect the glass transition temperatures of either types of sample: for epoxies $T_g = 263{\cdot}1\,\text{K} \pm 1{\cdot}4\,\text{K}$, for epoxy/liquid-crystal systems $T_g = 260{\cdot}2\,\text{K} \pm 0{\cdot}8\,\text{K}$. The three degree depression of T_g indicates that the liquid crystal is indeed acting as a plasticizer, but the small cure temperature dependence suggests that the glass transition is not a sensitive measure of the amount of liquid crystal in the matrix (and hence, by difference, the amount in the droplets).

Nevertheless, it is instructive to determine values of α from T_g for comparison with those found from ΔH_{NI}. It is straightforward to modify equation (3) to obtain the following expression

$$\alpha = 1 - F(T_{g2}/T_{g1})[(T_{g1} - T_g)/(T_g - T_{g2})], \quad (4)$$

where, as before, F is the ratio of polymer mass to liquid crystal mass in the sample, and subscript 1 refers to the polymer and subscript 2 to the liquid crystal. For the

sample densities and volume fractions in table 1. Equation (4) becomes

$$\alpha = 1 - 1{\cdot}74[(T_{g1} - T_g)/(T_g - T_{g2})]. \quad (5)$$

Values of α derived from equation (5) are plotted in figure 17 along with those from ΔH_{NI}. The values derived from T_g are much less sensitive to cure temperature than those from transition enthalpy. We believe the enthalpy-based results are more reliable, primarily because the simple version of the Gordon–Taylor equation (3) does not include a normalization coefficient which takes account of volumetric expansion [15, 17]†.

4.3. *Purity estimation of liquid crystal in microdroplets*

As discussed above (§ 4.1 (2)), some polymer precursor material is retained in the liquid crystal as an impurity after cure. This results in a depression of the clearing point temperature. We would like to be able to determine the impurity level of a PDLC system from the clearing point depression, using the same methods applied to depression of melting points. For melting, one uses the van't Hoff analysis [18, 19] for eutectic-forming systems, in which the fraction, f, of sample melted is determined as a function of temperature. From a plot of $1/f$ vs. temperature, the mole fraction of impurity is determined. The relevant equation is

$$T = T_0 - (RT_0^2\beta)/(f\Delta H), \quad (6)$$

where T is the temperature at which a fraction f of the sample has melted, T_0 is the true melting temperature, R is the molar gas constant, β is the mole fraction impurity, and ΔH is the molar enthalpy of melting.

Unfortunately, nematic–isotropic transitions fail the first and most important of the four assumptions upon which the van't Hoff analysis is based. The assumptions leading to equation 6 are [18, 20]: (1) The initial state of the system about to undergo the phase transformation is a mechanical mixture of the two phases—the majority and minority (impurity) phases. (Many impure crystals satisfy this assumption since the impurity often is included as a separate crystalline phase rather than being dissolved in the majority component as a solid solution. Impure liquid crystals obviously fail this criterion.) (2) The final state is an ideal solution. (Liquid crystal mixtures may approximate ideal behaviour.) (3) The transition enthalpies (latent heats) are temperature-independent. (This may be approximately true for liquid crystals; this assumption is not regarded as carrying the same weight as the first two.) (4) The impurity level is not too high (10 molar per cent is regarded as an upper limit).

In spite of the difficulties discussed in the previous paragraph, it is nevertheless instructive to estimate impurity level using the van't Hoff analysis. The result should give at least a rough idea of the degree of purity of the liquid crystal in the microdroplets. A more accurate assessment of purity could probably be based on the theory for the melting behaviour of ideal ascending solid solutions [21], but that treatment is rather complicated and would not yield closed-form expressions analogous to equation (6). Marti [22] has extensively reviewed calorimetric purity determinations for both eutectic and solid solution-forming systems. He points out that equation (6) can be corrected for solid solution formation by use of a partition coefficient, K,

† In the present work, we have insufficient information to evaluate the normalization coefficient.

the ratio of the concentrations of the *known* impurity in the solid and liquid phases (or in our case in the liquid crystal and liquid phases). We, of course, have no way to estimate K, and the impurities are not known. Marti points out that the use of equation (6), uncorrected for solid solution formation, can lead to a sizeable underestimation of impurity level (by as much as a factor of 7 or 8).

In the D.S.C. purity determination based on the van't Hoff analysis, it is necessary to make a semi-empirical 'x-correction' for peak area contributions which are undetectable due to noise considerations. The x-corrections needed for our PDLC systems were much larger (~ 37 to 46 per cent) than is usually acceptable. The large x-correction is probably not too surprising in view of the problems associated with using a nematic–isotropic transition rather than a melting point for the purity determination. In addition, the calculation requires a value of the liquid crystal molecular weight; since E7 is a mixture, an average value (260·2) was assumed. The large x-correction and the use of a mean molecular weight further add to our concerns regarding the validity of our purity estimates.

As expected, the analysis revealed that epoxy/liquid-crystal samples cured at lower temperatures were more impure than those cured at higher temperature. The impurity levels derived from equation (6) ranged from 0·5 mole per cent for a sample cured at 350 K to 0·3 mol per cent for one cured at 425 K. Of course, these derived purity levels are considerably suspect for the reasons discussed above. The true values of the impurity concentrations may actually be as much as an order of magnitude greater (~ 3 to 5 mole per cent). Although we reject the values of the impurity in the liquid crystal microdroplets found from the van't Hoff method, we believe that the trend toward higher purity with increasing cure temperature is correct.

4.4. *Ageing and post-cure effects*

The ageing and post-cure study results point out a problem which epoxies (and presumably other thermally cured systems) possess: changes in PDLC properties can take place with passing time or changing thermal environment. These properties changes presumably occur because the initial cure was incomplete and additional time or elevated temperature was required for additional crosslinks to form. The fact that ageing and post-cure increase T_g and T_{NI} without affecting ΔH_{NI} indicates that, as the degree of cure increased, the purity of the liquid crystal in the droplets also increased while the total amount in the droplets was unchanged. We have seen that a post-cure treatment at 400 K produced an increase in the clearing temperature to within a few degrees of that for the pure liquid crystal. Thus, it may be that such treatments would prove useful in enhancing desirable properties of thermally cured PDLC films.

We wish to thank D. B. Hayden for carrying out the SEM measurements of microdroplet size, T. H. Van Steenkiste for several useful modifications to the calorimeter, and W. D. Marion for technical assistance. Also we are grateful to J. W. Doane, J. L. West, R. T. Foister, J. P. Harris, W. R. Rodgers, W. T. Short, R. A. Basheer, Z. G. Gardlund, and G. P. Montgomery, Jr., for valuable discussions.

Notes added in proof.—(1) Cure time constant could alternatively be defined as that time by which $(1 - e^{-1})$ [$= 0{\cdot}632$] of the total heat of cure is released. A replot of figure 16 using this quasi-exponential time constant does not change the essential features of the figure. (2) An alternative explanation of the increase of T_{NI} for higher cure temperatures may be that lighter components of E7 are preferentially retained

in the polymer matrix at high T_{cure}, thus leaving in the microdroplets a liquid crystal mixture with a more elevated T_{NI}. (3) Our initial experiments with a U.V. cured PDLC clearly show that microdroplet size increases with increasing cure time constant for this system as well.

References

[1] DOANE, J. W., VAZ, N. A., WU, B. G., and ZUMER, S., 1986, *Appl. Phys. Lett.*, **48**, 269. See also DRZAIC, P. S., 1986, *J. appl. Phys.*, **60**, 2142.

[2] VAZ, N. A., SMITH, G. W. and MONTGOMERY, G. P., JR., 1987, *Molec. Crystals liq. Crystals*, **146**, 1.

[3] VAZ, N. A., SMITH, G. W., and MONTGOMERY, G. P., JR., 1987, *Molec Crystals liq. Crystals*, **146**, 17.

[4] MONTGOMERY, G. P., JR., and VAZ, N. A., 1987, *Appl. Optics*, **26**, 738.

[5] VAZ, N. A., and MONTGOMERY, G. P., JR., 1987, *J. appl. Phys.*, **62**, 3161.

[6] ROGINSKAYA, G. F., VOLKOV, V. P., CHALYKH, A. YE., AVDYEV, N. N., and ROZENBERG, B. A., 1980, *Effect of the Chemical Structure of Oligomer Rubbers on the Phase Equilibrium in Epoxy-Rubber Systems*, Polymer Science U.S.S.R., Vol. 21, p. 2331.

[7] LIPATOV, YU. S., GRIGOR'YEVA, O. P., KOVERNIK, G. P., SHILOV, V. V., and SERGEYEVA, L. M., 1985, *Makromol. Chem.* **186**, 1401.

[8] BDH Chemicals Ltd, Poole, England.

[9] SMITH, G. W., 1987, *Thermochim. Acta*, **112**, 289.

[10] FOISTER, R. T., 1986 (private communication).

[11] HARRIS, J. P., 1986 (private communication).

[12] SCHIRALDI, A., 1985, *Thermochim. Acta*, **96**, 283.

[13] ARMITAGE, D., and PRICE, F. P., 1976, *Chem. Phys. Lett*, **44**, 305.

[14] Present work, D.S.C. measurement.

[15] GORDON, M., and TAYLOR, J. S., 1952, *J. appl. Chem.*, **2**, 493.

[16] BRENNAN, W. P., 1973, *Thermal Analysis Applications Study No. 7*, Perkin-Elmer Corp., Norwalk, Connecticut. Brennan, W. P., 1973, *Thermal Analysis Applications Study*, No. 11, Perkin-Elmer Corp., Norwalk, Connecticut.

[17] MANZIONE, L. T., GILLHAM, J. K. and MCPHERSON, C. A., 1981, *J. appl. Polym. Sci.*, **26**, 907.

[18] PALERMO, E. F., and CHIU, J., 1976, *Thermochim. Acta*, **14**, 1. See also *Thermal Analysis Newsletters*, Nos. 5 and 6, Perkin-Elmer Corp., Norwalk, Connecticut.

[19] GRAY, A. P., 1972, *Thermal Analysis Application Study*, No. 3, Perkin-Elmer Corp., Norwalk, Connecticut.

[20] SMITH, G. W., 1977, *Molec Crystals liq. Crystals*, **42**, 307.

[21] SMITH, G. W., 1981, *Molec. Crystals liq. Crystals*, **65**, 285.

[22] MARTI, E. E., 1972, *Thermochim. Acta*, **5**, 173.